

Structural Properties of Chemically-Deposited ZnO_xS_{1-x} Solid Solutions

T.O. Berestok^{1*}, A.S. Opanasyuk¹, N.M. Opanasyuk¹, Yu.P. Gnatenko²

¹ Sumy State University, 2, Rymtsky Korsakov Str., 40007 Sumy, Ukraine

² Institute of Physics of National Academy of Sciences of Ukraine, 03028 Kyiv, Ukraine

(Received 19 June 2014; published online 29 August 2014)

In paper, by the methods of scanning electron microscopy and X-ray diffraction there are investigated the structural features of films of ZnO_xS_{1-x} solid solutions, which are deposited from solutions of zinc acetate, thiourea and ammonia. As a result, the influence of deposition time on the elemental and phase composition of thin films and their structural characteristics are studied. It is established that increasing time of deposition of the films leads to an increase of sulfur concentration in their composition from 9.86 at. % to 14.06 at. %. It is shown that all condensates have hexagonal structure with lattice constants of $a = 0.32486$ nm, $c = 0.52086$, $c/a = 1.603$, and growth texture of [200], the quality of which depends on the deposition time.

Keywords: ZnO_xS_{1-x}, Chemical bath deposition, X-ray diffraction, Morphology, Structural studies.

PACS numbers: 81.05.Dz, 61.46.Km

1. INTRODUCTION

ZnO_xS_{1-x} solid solutions have attract a great attention of researchers because of the possibility of band gap engineering in the material in a wide range of energies from 3.37 eV (ZnO) to 3.68 eV (ZnS), depending on the content of S [1]. This allows to create an effective ultraviolet photodetectors, gas sensors, electroluminescent devices. [2]. The authors of [3] showed that introduction of sulfur in ZnO condensates improves the efficiency of luminescence, which makes it possible to create efficient phosphors based on this material. The use of ZnO_xS_{1-x} window layers instead of ZnO can also increase the efficiency of thin films solar cells on the basis of absorbing films of CdTe, Cu(In, Ga)Se₂ and Cu₂ZnSnS₄ [4,5] by increasing their transmission in the ultraviolet region of the spectrum.

Traditionally, ZnO_xS_{1-x} solid solutions are obtained using high-vacuum techniques such as the method of gas transport reactions [6] radio-frequency (RF) reactive sputtering [7], magnetron sputtering [8], pulsed laser deposition [9]. These techniques are technically difficult and uneconomic, which significantly increases the cost of creating device based on them. In addition in layers obtained by pulsed laser deposition authors [10] registered extraneous phase formation of ZnSO₄, which is unacceptable in the future use of films in electronics.

Unlike the known work for obtaining of ZnO_xS_{1-x} solid solutions we used the method of chemical bath deposition from an aqueous solution (CBD) [11], which is simple, economical; also it is possible to get condensates with predicted structural properties - continuous films, nanodots, nanowires, nanorods [12-13].

Since the structural properties of ZnO_xS_{1-x} films were studied insufficiently, we've made an investigation of the influence of physical and chemical conditions of synthesis on the texture quality, the values of the lattice constants, the size of coherent scattering domains (CSD).

2. EXPERIMENTAL DETAILS

Obtaining of ZnO_xS_{1-x} layers was carried out by chemical bath deposition from aqueous solution of zinc acetate (Zn(O₂CCH₃)₂) and thiourea (CS(NH₂)₂). To maintain a pH of 10, we added ammonia solution to the initial mixture. As the substrate for film deposition there was used a glass with FTO (SnO₂: F) underlayer, which was pre-cleaned in isopropanol for 20 min using an ultrasonic generator. During the synthesis the temperature of chemical reactor was maintained at 90 °C. For obtaining of different thickness of the layers, duration of deposition was varied in the range from 30 to 120 minutes. In some cases after the deposition, synthesized condensates were annealed at $T = 450$ °C in an atmosphere of sulfur.

Surface morphology of the samples was studied using a scanning electron microscope of Zeiss Auriga Cross Beam. The chemical composition of synthesized films was determined by energodispersive analysis (EDAX) using X-ray detector of scanning electron microscope.

Structural studies of the layers have been performed by automated X-ray diffractometer of Bruker D8 Advance in Ni-filtered of K_{α} radiation of copper anode. The spectra were registered in the angle range 2θ from 20° to 80°, where 2θ is the Bragg angle.

Obtained X-ray patterns were normalized by (100) peak of hexagonal phase of ZnO. Texture quality of the films was estimated by the method of Harris, which is especially convenient for testing flat samples with the axis of the texture that is oriented normal to the surface [14-15]. Pole density was calculated according to the equation:

$$P_i = \frac{(I_i/I_{0i})}{\frac{1}{N} \sum_{i=1}^N (I_i/I_{0i})}, \quad (1)$$

* taisia.berestok@ukr.net

where I_i , I_{oi} are integral intensity of the i -th diffraction peak of the film samples and etalon; N is the number of lines present in the diffractogram.

Then we built dependences of $P_i - (hkl)_i$ and $P_i - \varphi$, where φ is an angle between the axis of the texture and perpendicular to the different crystallographic planes, which are responsible to the reflections in the diffractograms, (hkl) are Miller indices. This angle is calculated for hexagonal phase using the expressions given in [14].

Texture axis has the index, which corresponds to the largest value of P_i . In this case, the orientation factor for the relevant direction can be calculated from the formula

$$f = \sqrt{\frac{1}{N} \sum_{i=1}^N (P_i - 1)^2}. \quad (2)$$

Determination of interplanar distances, found in the samples, was carried out by the position of K_{a1} component of all of the most intense lines presents in the X-ray diffraction patterns.

Calculation of the lattice constants, a and c of the hexagonal phase in the films was carried out using equations:

$$a = \frac{\lambda}{2 \sin \theta} \sqrt{\frac{4}{3} (h^2 + hk + k^2) + \left(\frac{a}{c}\right)^2 l^2}, \quad (3)$$

$$c = \frac{\lambda}{2 \sin \theta} \sqrt{\frac{4}{3} \left(\frac{c}{a}\right)^2 (h^2 + hk + k^2) + l^2}, \quad (4)$$

where λ is wavelength of X-rays.

During the calculations, the ratio of c/a was considered equal to the value characteristic for the ideal unit cell of wurtzite of 1.601.

Further to obtain precise values of the lattice constants we used an extrapolation method of Nelson-Riley [15]. The linear approximation of points was performed using a least squares method.

XRD results were also used to determine the average size CSD (L). Their size in chalcogenide films, was estimated by Scherrer's equation [14]:

$$L = \frac{K\lambda}{\beta \cos \theta}, \quad (5)$$

where K is a coefficient that depends on the shape of the grain ($K = 0.94$); β is a physical broadening of the diffraction lines.

3. RESULTS AND DISCUSSION

Surface images of obtained $\text{ZnO}_x\text{S}_{1-x}$ condensates before and after annealing are presented in Figure 1

As it can be seen from the Figure, after deposition for 30 min (Fig. 1) the islands of solid solution were formed on the substrate; increasing of the duration of deposition to 60 min (Fig. 1 b) leads to filling the intervals between them, and condensation for 120 min - to formation of a highly porous labyrinth structures (Fig. 1 c).

Annealing of synthesized condensates (Fig. 1 d) at $T = 450^\circ\text{C}$ in an atmosphere of sulfur leads to coalescence of nanodots with a diameter of 0.5-0.7 microns in porous aggregates.

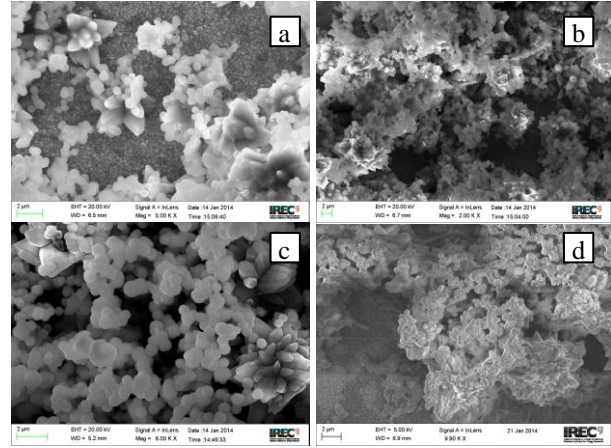


Fig. 1 - SEM images of fresh-deposited $\text{ZnO}_x\text{S}_{1-x}$ condensates at different deposition time t , min: 30 (a); 60 (b); 120 (c) and films after annealing at deposition time of 60 min (d)

Fig. 2 shows the EDAX spectra of condensates synthesized for the duration of deposition of 60 min before (Fig. 2 a) and after annealing (Fig. 2 b). As it can be seen from the Figure, except the elements belonging to the $\text{ZnO}_x\text{S}_{1-x}$ films, because investigated films were thin and highly porous, we registered the extraneous elements which belong to FTO substrate.

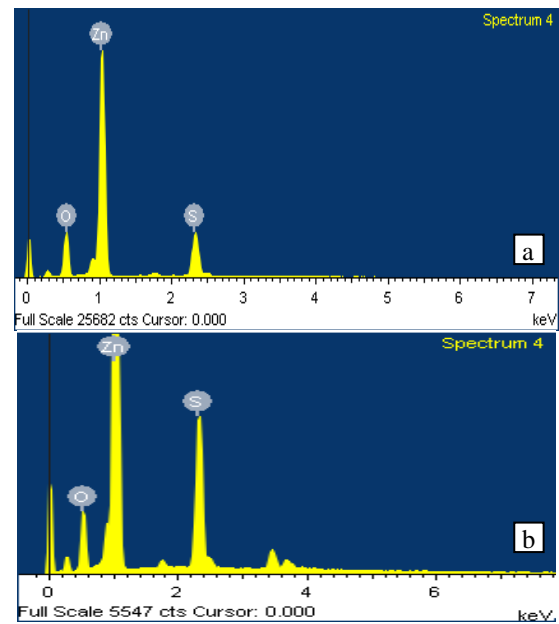


Fig. 2 – Typical EDAX spectra of obtained films at duration of 60 min before (a), and after annealing (b) in S atmosphere

Table 1 displays the results of determination of the elemental composition of the layers by EDAX. It is shown, that with increasing deposition time of the layers, atomic concentration of sulfur increases. A similar effect we fixed in the samples after annealing in an atmosphere of sulfur.

In the XRD patterns (Fig. 3) we have registered intense peaks at the angles of 31.85° , 36.35° , 66.55° , which were shifted relative to the position of reflections from planes of (100), (101), (200) of ZnO hexagonal phase.

Table 1 – Elemental composition of synthesized condensates ZnO_xS_{1-x} used different deposition time before and after annealing

Concentration C , at. %	τ , min			
	Before annealing			After annealing
	30	60	120	60
O	61,35	58,25	22,79	41,10
S	9,86	12,26	14,06	20,66
Zn	28,79	29,49	63,15	38,24

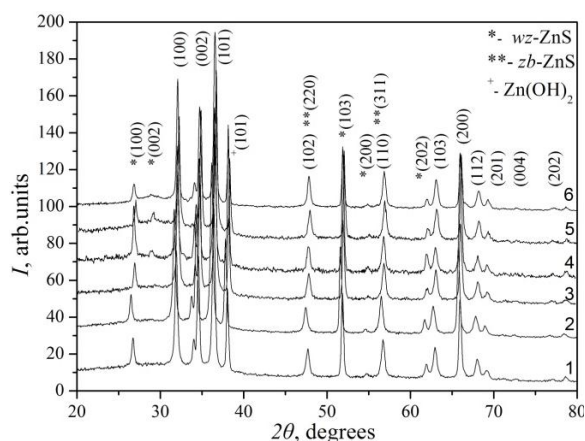


Fig. 3 – Diffraction patterns of ZnO_xS_{1-x} condensates at different duration τ : 1 – 30 min; 2 – 45 min; 3 – 60 min; 4 – 90 min; 5 – 120 min; 6 – 60 min (after annealing)

This indicates the formation of ZnO_xS_{1-x} solid solution with hexagonal modification, which has values of lattice constant a , c different from ZnO ones. Also, fairly intense lines corresponding to the reflection from planes of (100), (002), (103) of zinc sulfide with wurtzite structure are presented in X-ray patterns.

Furthermore we have registered peak from $Zn(OH)_2$ phase at small angles in some XRD patterns [18, JCPDS 002-124]. It may be the result of incorporation of atoms from precursors during chemical reactions in the crystal lattice of the condensate. Analysis of the literature shows that vacuum annealing of obtained layers leads to decomposition of this compound [19].

Pole density estimation of synthesized solid solutions showed that the condensates have weak ($f = 1.94 - 2.30$ arb.units) axial growth texture [200]. This texture is not typical for zinc oxide films, where, basically, we observe growth texture of [002] [20]. Changing of growth texture in the films can be the result of incorporation of sulfur atoms in the crystal structure of ZnO. As it shown in Fig. 4 growth texture quality of condensates weakly depends on the duration of deposition.

Fig. 5 shows the dependence of deposition time on the lattice constants values of the material. In the figure the dotted line marked reference data correspond to ZnO [18, JCPDS 79-0205].

As you can see from the Figure, the values of the lattice constants of the thick layer ($\tau = 60-120$ min) exceed the reference values of ZnO. Apparently it is due to the presence of sulfur atoms in the films, the concentration of which increases during the synthesis.

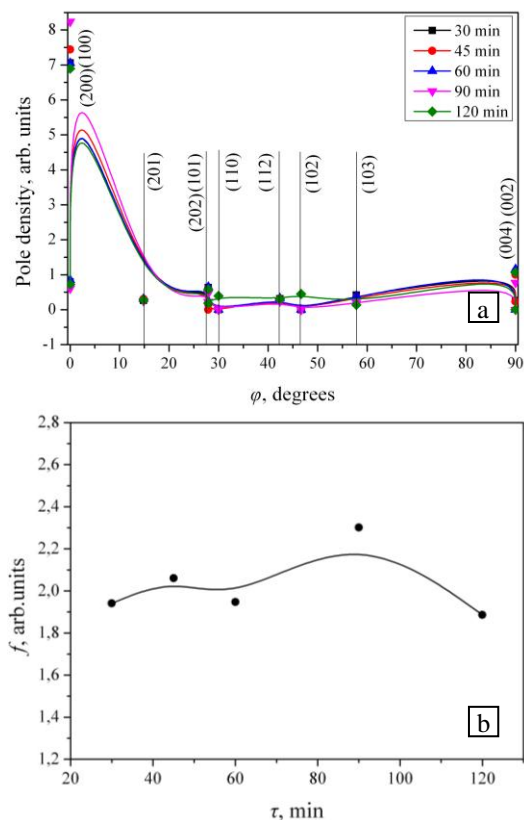


Fig. 4 – Dependence of the pole density P_i on the angle φ between the texture axis and the normal to the reflection plane at different duration (a) and the orientation factor dependence (b)

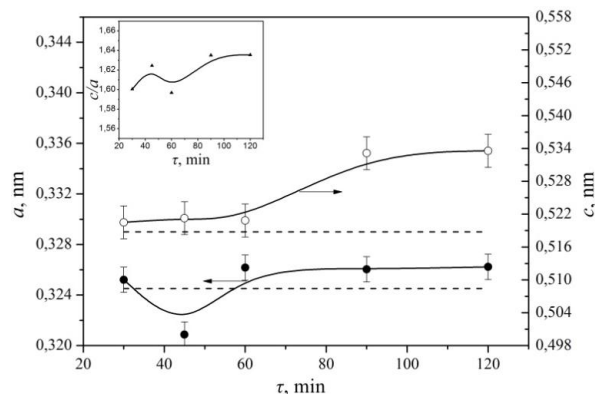


Fig. 5 – Dependence of the lattice constants a and c and the ratio c/a (in the inset) on the condensation time

Dependencies of coherent scattering domain size in the direction perpendicular to crystallographic planes of (002), (101), (100), obtained using the equation (5), are shown in Fig. 6.

It is established that the values of coherent scattering domain size (CSD) L practically don't change in all crystallographic direction for various deposition time. The values of CSD are in the range of $L_{(100)} = (32.8-33.1)$ nm, $L_{(002)} = (35.5-36.0)$ nm, $L_{(101)} = (37.6-38.0)$ nm. These values are smaller than electron-defined. This indicates that the crystallites contain of several sub-grains.

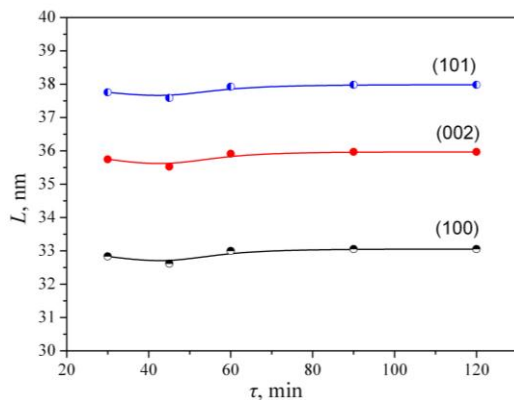


Fig. 6 – Effect of duration of the films on the coherent scattering domain size

4. CONCLUSION

Investigated layers of ZnO_xS_{1-x} solid solutions were synthesized by the method of chemical bath deposition from an aqueous solution of zinc acetate, thiourea and ammonia with different condensation time. Investigation of surface morphology of the samples showed that the process of nanodots formation is occurred on the substrates. Increasing of the deposition time leads to splice the gaps between nanodots and the formation of porous structures. Annealing of the condensates leads to coalescence of nanodots in porous aggregates.

It was established that the increase of deposition time of the films leads to an increase of the concentra-

tion of sulfur in their composition from 9.86 at. % to 14.06 at. %; annealing in an atmosphere of sulfur of the condensates leads to increase of S content to 20.66 at. %.

It is shown that the synthesized layers have hexagonal structure with growth texture of [200], the quality of which is weakly dependent on film thickness.

With increasing time of films deposition due to increase of sulfur concentration, the effect of increasing of lattice constants values of ZnO_xS_{1-x} solid solution (from $a = 0.32087$ nm to $a = 0.32623$ nm, and from $c = 0.52051$ nm to $c = 0.53356$ nm) was found in the layers.

Estimating of CSD values showed that the crystallite size does not depend on the deposition time of condensate. Values of CSD are in the range of $L_{(100)} = (32.8-33.1)$ nm, $L_{(002)} = (35.5-36.0)$ nm, $L_{(101)} = (37.6-38.0)$ nm.

It was found that chemically-synthesized ZnO_xS_{1-x} solid solutions can be used to create new optoelectronic devices with improved characteristics.

ACKNOWLEDGEMENTS

This research was supported by the Ministry of Education and Science of Ukraine (Grant No. 0113U000131 and 0112U000772).

The authors are thankful to the Functional Nanomaterials group and Catalonia Institute for Energy Research for the assistance in researches.

REFERENCES

- H. Che, J. Huso, J. L. Morrison, D. Thapa, M. Huso, W. J. Yeh, M. C. Tarun, M. D. Mc Cluskey, L. Bergman, *J. of Nanomat.* **1**, 1 (2012).
- R.N. Bhargava, D. Haranath, A. Mehta, *J. of the Korean Phys. Soc.* **53**, No. 5, 2847 (2008).
- Y. He, L. Zhang, L. Wang, M. Li, X. Shang, X. Liu, Y. Lu, B. K. Meyer, *J. of Alloy. Compd.* **587**, 369 (2014).
- M. Ameri, D. S. Eddine, M. Sebane, K. Boudia, Y. Al-Douri, A. Bentouaf, D. Hachemane, B. Bouhaf, A. Touia, *Mater. Sci. and Appl.* **4**, 63 (2013).
- X.F. Fan, Z.X. Shen, Y.M. Lu, J.L. Kuo, *New J. Phys.* **11**, 093008 (2009).
- S. Locmelis, C. Brunig, M. Binnewies, A. Borger, K.D. Becker, T. Homann, T. Bredow, *J. Mater. Sci.* **42**, 1965 (2007).
- Y. He, L. Zhang, L. Wang, M. Li, X. Shang, X. Liu, Y. Lu, B. Meyer, *J. of Alloy. Compd.* **534**, 81 (2012).
- B.K. Meyer, A. Polity, B. Farangis, Y. He, D. Hasselkamp, Th. Kramer, C. Wang, *Appl. Phys. Lett.* **85**, 4929 (2004).
- Y.Z. Yoo, Zh.W. Jin, T.S. Chikyow, *Appl. Phys. Lett.* **81** No 20, 3798 (2002).
- R. Zhang, B. Wang, L. Wei, *Vacuum* **82**, 1208 (2008).
- T.O. Berestok, D.I. Kurbatov, A.S. Opanasyuk, N.M. Opanasyuk, V.M. Kuznetsov, *22 nd Int. Crimean Conf "Microwave and Telecommunication Technology"(CriMiCo'2012), art. No CFP12788, 693* (Sevastopol: Veber:2012).
- A.S. Opanasyuk, T.O. Berestok, P.M. Fochuk, A.E. Bolotnikov, R.B. James *Proc. of SPIE* **8823**, 88230Q-1 (2013).
- Ja. S. Umanskij, Ju. A. Skakov, A. N. Ivanov, L. N. Rastorguev, *Crystallography, X-ray graph and electronmicroscopy*, (Moscow, 1982). (in Russian)
- B.E. Warren, *X-ray Diffraction. Dover Books on Physics*, (New York, 1990).
- V.V. Kosyak, D.I. Kurbatov, M.M. Kolesnyk, A.S. Opanasyuk, S.N. Danilchenko, Yu.P. Gnatenko, *J. Mater. Chem. Phys.* **138**, 731 (2013).
- S. Ilican, Y. Caglar, M. Caglar, *J. Optoelectron. Adv. M.* **10** No 10, 2578 (2008).
- U. Seetawan, S. Jugsuginda, T. Seetawan, A. Ratchasin *Mater. Sci. Appl.* **2**, 1302 (2011).
- Selected powder diffraction data for education straining (Search manual and data cards), Published by the International Centre for diffraction data, 432 (1997). JCPDS# 79-0205.
- F. Long, W.-M. Wang, Zh. Cui, L. Fan, Zh. Zou, T. Jia, *Chem. Phys. Lett.* **462**, 84 (2008).
- T.O. Berestok, D.I. Kurbatov, N.M. Opanasyuk, A.D. Pogrebnjak, O.P. Manzhos, S.M. Danilchenko, *J. Nano-Electron. Phys.* **5** No 1, 01001 (2013).